PERGAMON

International Journal of Heat and Mass Transfer 42 (1999) 3631–3641

International Journal of HEAT and MASS TRANSFER

www.elsevier.com/locate/ijhmt

The temperature distribution and heat transfer in anisotropic electromechanical converter

D. Spałek*

Technical University of Silesia, Gliwice Institute of Theoretical and Industrial Electrotechnics, Akademicka 10 St, PL-44-100 Gliwice, Poland

Received 11 August 1998; received in revised form 15 December 1998

Abstract

The electromagnetic and thermal fields for some types of electromechanical converters under steady-periodic state regime have been determined analytically. The magnetic potential and temperature field equations, in terms of cylindrical coordinates have been solved for the steady-periodic state work-load case. The magnetic as well as the thermal parameters of the converters considered are linear and indicate the anisotropic features.

1. Introduction

When running, the various parts of an electromechanical converter (that is an electrical machine) will exhibit temperature rises due to the flow of stator and rotor currents. The problem of determining what these rises are likely to be, in practice, is very difficult, but nevertheless, very important both for machine constructors and their end users. The experimental approach, i.e. the direct determination of the temperature rises, is hampered by the great variation in size of typical electrical machines with solid rotors. Thus, on the one hand, one has the huge power-station generators whilst on the other, one has the small to tiny asynchronous machines which are used in actuators or in positioning systems. This makes a theoretical approach attractive even though this involves the estimation of the spatial variation of both the electromagnetic and the temperature fields. This paper presents analytical analyses for two important cases:

1. synchronous 3-phase generators with cylindrically shaped solid rotors operating under asynchronous working conditions;
2. 2-phase asynchronous machines operating under nominal work conditions.

The industrial production methods for the rotors of these machines involve layered structures which necessarily involve anisotropy for both the electromagnetic and the thermal parameters. The usual way of investigating such anisotropic systems is to use numerical methods such as FEM, BEM [2,9] but it is also possible, without too much difficulty, to use purely analytic approaches as well [2]. These analytical methods have the great advantage that one can readily and quickly investigate the effects of changes of geometry and/or material properties and thus plot graphs etc without needing resource to expensive computer time. Particular examples of important machine parameters whose influence can be studied analytically include magnetic permittivity, specific heat, convection coefficient etc. Another great merit of the analytical approach is that it provides a way of checking the

* Tel.: +48-32-237-1258; fax: +48-32-327-1258.
E-mail address: dspalek@zeus.polsl.gliwice.pl (D. Spałek)

0017-9310/99/$ - see front matter
PII: S0017-9310(99)00035-6

Nomenclature

a	conducting layer width
a_a, b_a, a_δ, b_δ	constants for solutions of differential equations for magnetic field
a_θ, b_θ	constants for solutions of differential equations for temperature
$\vec{A}$	the magnetic vector potential; it defines both electric and magnetic field [4] as follows, $\vec{E} = -\mathrm{A}\rightarrow$, $\vec{B} = \mathrm{curl}(\vec{A})$
$\mathbf{A}(r)$	matrix of set differential equation
B_r, B_α	magnetic flux density components, $B_r = \partial A/r\partial\alpha$, $B_\alpha = -\partial A/\partial r$,
$Bi = \alpha_f R/\lambda_{rr}$	Biot number
c_p	specific heat
c_1, c_2	constants for temperature $\vartheta(r)$
$\mathbf{C}_o$, $\mathbf{C}(r)$	denote constant and function for solutions of Bessel's equation
$\vec{E}$	electric field strength, $\vec{E} = -\mathrm{A}\rightarrow$
f	frequency of rotor currents
f_s	frequency of stator currents
g	the gap width
$i = \sqrt{-1}$	imaginary unit
$\vec{\imath}_r$, $\vec{\imath}_\alpha$, $\vec{k}$	radial, tangential and axial unit vectors, respectively
$\vec{j} = \gamma\vec{E}$	current density
$I_1(r)$, $I_2(r)$	auxiliary integrals
$I_{pB}(\beta r)$, $K_{pB}(\beta r)$	modified Bessel's functions
$k(r) = (\kappa^2 + p_T^2 r^{-2})$	parameter of Bessel's equation
p	the pole pair number
$\Delta p(r, x)$	local power losses volume density
p_B, p_T	orders of Bessel's functions $p_B = p\frac{\sqrt{\nu_{rr}}}{\nu_{\alpha\alpha}}$, $p_T = p\frac{\sqrt{\lambda_{\alpha\alpha}}}{\lambda_{rr}}$
P, Q	auxiliary constants
$P(r)$, $\Delta P(r)$	power losses density
$\mathbf{P}(r)$	auxiliary vector
r	radius or the radial coordinate
R	outer radius of the layer
$R(r)$, $S(\alpha, t)$	functions separated
S_+, $S_- = S$	constants of $S(\alpha, t)$
$s = i\omega$	imaginary angular speed
$T(r, \alpha, t)$	temperature
T_f	fluid temperature in the gap
U, W	auxiliary constants
$\mathbf{W}(r)$	Wronsky's matrix
$x = \omega t - p\alpha$	angular-time variable
$\mathbf{X}(r)$	vector of temperature and its radial derivative
$Z(\beta r) = a_a I_{pB}(\beta r) + b_a K_{pB}(\beta r)$	auxiliary function for current density

Greek symbols

α	angular coordinate
α_f	convection coefficient
$\beta = \sqrt{s\gamma\nu_{\alpha\alpha}^{-1}}$	skin effect parameter
γ	electric conductivity of the rotor layer
ϵ_o	dielectric permittivity for the vacuum
ϑ, θ	temperature components
θ_r, θ_s	rotor and stator mmfs $\kappa = \sqrt{2i\omega\rho c_p\lambda_{rr}^{-1}}$
$\lambda_{\alpha\alpha}$, λ_{rr}	thermal conductivities
ν_o, ν_{rr}, $\nu_{\alpha\alpha}$	magnetic reluctivity for the air-gap and the rotor layer, respectively
ρ	mass density
$\omega_s = 2\pi f_s/p$	angular stator speed
$\omega = 2\pi f/p = \omega_s - \Omega_m$	rotor current angular speed
Ω_m	rotor mechanical speed

quality of the numerical solutions. It should also be pointed out that the experimental approach, which at first sight might be thought to be preferable, can be very expensive and time consuming yet still not give trustworthy results mainly due to the lack of accurate values for the material parameters. Numerical solutions would therefore be needed over a wide-range of these parameters in order for a design engineer to be sure that the machine will perform to specification under all likely operational conditions. Analytical solutions can therefore be very attractive.

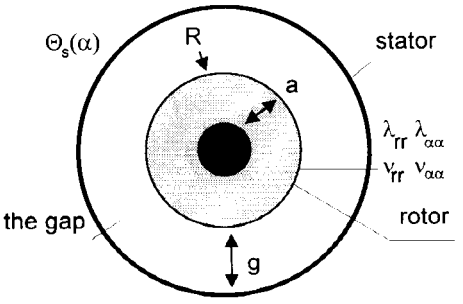

Fig. 1. Exemplary electromechanical converter cross-section.

2. A model electromechanical converter

The model investigated is constructed with the following assumptions. The symmetry is assumed to be axially-symmetric i.e. cylindrical so that both fields can be specified using simple polar coordinates in the plane perpendicular to the axis. The material properties are assumed to have the normal (diagonal) anisotropy [7] and these properties are assumed to be linear. Three distinct regions are considered; the gap, the anisotropic layer and the ferromagnetic rotor core. The air-gap electromagnetic parameters are like for the vacuum. The medium temperature T_f in the air-gap is known as well as the convection coefficient α_f between the air-gap and the outer surface of the rotor. The conducting layer presents the diagonal anisotropy of magnetic and thermal parameters. The rotor inner part of electromechanical converter (the so-called core—the black one in Fig. 1) has the zero magnetic reluctivity. The core and the anisotropic layer are insulated from each other for not conducting both the electric current and heat flux. The currents led in stator winding are distributed along the periphery of the machine having the so-called p-pole symmetry. The cross-section of electromechanical converter is shown in Fig. 1.

The parameters for all regions are grouped in Table 1.

The solution of electromagnetic field equation has been received considering the stator and rotor currents values. The currents and the boundary conditions for magnetic field components result from the magnetic field distribution. The total magnetic field, which appears in conducting rotor, forces the spatial distribution of rotor eddy currents. According to Joule's principle the power losses volume density have been evaluated. The heat transfer equation and boundary conditions for heat flux constitute the analytical solution for temperature field distribution. The distribution of temperature and heat flux is known if all constant of solutions would be calculated due to values assumed of the mmf and the material parameters.

3. Electromagnetic field

The determination of the electromagnetic field is carried out under the following assumptions:

- 2-D analysis ($\partial/\partial z = 0$) of field distribution

$$\vec{H} = \nu_{rr}\vec{B}_r + \nu_{\alpha\alpha}\vec{B}_\alpha, \quad \vec{E} = -\frac{\partial \vec{A}}{\partial t} = -\vec{k}\dot{A}. \tag{1}$$

$$\vec{B} = \mathrm{curl}\vec{A} = \vec{\imath}_r \frac{1}{r}\frac{\partial A_z}{\partial \alpha} - \vec{\imath}_\alpha \frac{\partial A_z}{\partial r}, \tag{2}$$

- the electric displacement current is omitted,
- the 2p-pole space distribution of the mmf (the magnetomotive force is created by the stator windings

Table 1
Electromagnetic and thermal parameters (SI units)

Region/parameters	Electromagnetic	Electric	Thermal	The forced
$(R, R+g)$ gap	$\nu_o = (1/4\pi) \cdot 10^7$ H m^{-1}	$\epsilon_o = 8.85 \cdot 10^{-12}$ F m^{-1}	–	α_f, T_f θ_s, p
$(R-a, R)$ layer	$\nu_{\alpha\alpha}$, ν_{rr} γ	ϵ_o, γ $\epsilon_o\omega\gamma^{-1} \to 0$	$\lambda_{\alpha\alpha}$ λ_{rr}	Ω_m
$(0, R-a)$ core	$\nu_{Fe} = 0$	–	$\lambda_{Insulation} \to 0$	–

and means the current under one pair-pole) is given by [3]

$$\theta_s(\alpha) = \theta_s \cos(2\pi f_s t - p\alpha + \pi/2) = \theta_s \operatorname{Re}\{\exp[i(2\pi f_s t - p\alpha + \pi/2)]\}.$$

The pair-pole number $p>0$ generates the variation of currents in rotor vs angular coordinate α. Since $p=0$ the currents density in cylindrical rotor depends only on the radial coordinate r.

- there exists the normal cylindrical anisotropy of magnetic reluctivities for rotor $\nu_{rr}-\nu_{\alpha\alpha}\neq 0$.

The Maxwell's equation [4] in the form well-known (for the conducting region since frequency $f \ll 10^{17}$ Hz)

$$\operatorname{curl}(\vec{H}) = \gamma \vec{E}, \tag{3}$$

leads to partial differential equation which governs the magnetic vector potential distribution as follows

$$\nu_{\alpha\alpha}\frac{1}{r}\frac{\partial}{\partial r}\left(r\frac{\partial A}{\partial r}\right) + \nu_{rr}\frac{1}{r^2}\frac{\partial^2 A}{\partial \alpha^2} = -\gamma \dot{A}. \tag{4}$$

The Eq. (4) is analogous to the well-known Fourier equation. The partial time derivative under steady-periodic state regime could be represented in terms of the operand $i\omega$ and the complex magnetic potential as follows for the rotor

$$\frac{\partial}{\partial t}A \Longrightarrow i\omega A, \quad A(t) = \operatorname{Re}\{A \exp(i\omega t)\}.$$

The observer, which is connected with the stator, describes the magnetic potential multiplying it by the operand $e^{ip\Omega_m t}$, where Ω_m means the rotor angular speed. The Eq. (4) can be solved by the functions separation in the well-known form

$$A(r, t, \alpha) = R(r)S(t, \alpha). \tag{5}$$

Substituting the given above relation into Eq. (4) and separating both R and S function it can be written the following relations

$$\begin{cases} -\dfrac{1}{S}\dfrac{d^2 S}{d\alpha^2} = p^2 \\ \dfrac{\nu_{\alpha\alpha}}{\nu_{rr}}\dfrac{r}{R}\dfrac{d}{dr}\left(r\dfrac{dR}{dr}\right) - \dfrac{s\gamma r^2}{\nu_{rr}} = p^2 \end{cases}. \tag{6}$$

On the right-hand sides of both equations the square of pair-pole number p was used for obtaining at once the physical solutions adequate to the assumed space distribution of mmf. For the air-gap it should be assumed $\gamma=0$, $\nu_{rr}=\nu_{\alpha\alpha}=\nu_o$.

The first relation of the set (6) has the solution given by exponential function

$$S(t,\alpha) = S_- \exp(i\omega t - ip\alpha) + S_+ \exp(i\omega t + ip\alpha). \tag{7}$$

In order to obtain the physical solution it must be assumed (the rotating magnetic field caused by the mmf of symmetrical stator windings) $S_+ = 0$.

For the region of rotor layer, the second relation of the set (6) presents Bessel's equation of p_Bth order whose solution is given by modified Bessel's functions

$$R(r) = a_a I_{pB}(\beta r) + b_a K_{pB}(\beta r). \tag{8}$$

If p_B is not an integer number (for the anisotropic rotor, generally) thus the modified function $K_{pB}(\beta r)$ could be replaced by Bessel's function of negative order $I_{-pB}(\beta r)$.

For the anisotropic rotor layer (the auxiliary index a is used, $x = \omega t - p\alpha$) the magnetic flux density components are equal to

$$B_{ar} = \frac{p}{r}\{a_a I_{pB}(\beta r) + b_a K_{pB}(\beta r)\} \exp(ix) \tag{9}$$

$$B_{a\alpha} = -i\beta\{a_a I'_{pB}(\beta r) + b_a K'_{pB}(\beta r)\} \exp(ix). \tag{10}$$

For the air-gap ($\gamma=0$, $\nu_{rr}=\nu_{\alpha\alpha}=\nu_o$) the relations (6) lead to the solutions for the magnetic flux density components (this auxiliary index δ is used)

$$B_{\delta r} = \frac{p}{r}\{a_\delta r^p + b_\delta r^{-p}\} \exp(ix) \tag{11}$$

$$B_{\delta\alpha} = -pi\{a_\delta r^{p-1} - b_\delta r^{-p-1}\} \exp(ix). \tag{12}$$

The four constants, that appeared in Eq. (9)–(12), are usually evaluted basing on four boundary conditions (see Appendix, [4]). The boundary conditions given below enable one to determine all constants which appeared in Eq. (9)–(12). The distribution of the magnetic vector potential leads to the distribution of the eddy current density $j(r, x)$, power losses $\Delta p(r, x)$ and the temperature, subsequently.

4. Eddy currents and power losses

Having known the distribution of the magnetic field under the steady-periodic state, the spatial distribution of eddy current could be determined as follows

$$\begin{aligned} j(r, \alpha, t) &= -\gamma s A(r, \alpha, t) \\ &= -\gamma s A(x, r) = -\gamma s Z(r) \exp(ix). \end{aligned} \tag{13}$$

The magnetic vector potential is given by Eq. (9)–(12) and henceforth they result in both electric field strength and eddy current spatial density. The values of the eddy current losses

$$\Delta p(r,x) = \gamma^{-1}(\mathrm{Re}\{\, j(r,x)\})^2 = \frac{1}{2}\gamma^{-1}\,\mathrm{Re}\{j(r,x)j^*(r,x)\} + \frac{1}{2}\gamma^{-1}\,\mathrm{Re}\{j(r,x)j(r,x)\}, \tag{14a}$$

could be evaluated as follows

$$\Delta p(r,x) = P(r) + \mathrm{Re}\{\Delta P(r)\ \exp(2ix)\}, \tag{14b}$$

where it was denoted

$$P(r) = \frac{1}{2}\gamma^{-1}\mid j(r,0)\mid^2 = \frac{1}{2}\gamma\mid s\mid^2 Z(\beta r)Z^*(\beta r) = \mid \Delta P(r)\mid, \tag{15}$$

$$\Delta P(r) = \frac{1}{2}\gamma^{-1}j(r,0)^2 = \frac{1}{2}\gamma s^2 Z^2(\beta r). \tag{16}$$

The results of the eddy currents and local loses calculation for chosen material and geometrical parameter values are shown in Fig. 2 (SI units system). According to Fig. 2 it is apparent that the losses density varies with both the angular and radial co-ordinate, therefore it cannot be neglected.

5. Temperature field

The equation for temperature $T(r, \alpha, t)$ space–time distribution has the well-known form [5]:

$$\mathrm{div}(\vec{q}) + c_\mathrm{p}\rho\dot{T} = \Delta p, \tag{17}$$

where the heat flux is equal to

$$\vec{q} = -\lambda_{rr}\frac{\partial T}{\partial r}\vec{\imath}_r - \lambda_{\alpha\alpha}\frac{\partial T}{r\partial\alpha}\vec{\imath}_\alpha. \tag{18}$$

The equations written above constitute the differential equation for the temperature

$$\lambda_{rr}\frac{1}{r}\frac{\partial}{\partial r}\left(r\frac{\partial T}{\partial r}\right) + \lambda_{\alpha\alpha}\frac{1}{r^2}\frac{\partial^2 T}{\partial\alpha^2} - c_\mathrm{p}\rho\dot{T} = -\Delta p. \tag{19}$$

Eq. (19)—according to its linearity—can be split into two equations. On the right-hand side of the two brand-new equations obtained only one component either P or ΔP appears. The first equation derived has the written form below

$$\lambda_{rr}\frac{1}{r}\frac{\partial}{\partial r}\left(r\frac{\partial(\theta e^{2xi})}{\partial r}\right) + \lambda_{\alpha\alpha}\frac{1}{r^2}\frac{\partial^2(\theta e^{2xi})}{\partial\alpha^2} - c_\mathrm{p}\rho\frac{\partial}{\partial t}(\theta e^{2xi}) = -\Delta P e^{2xi}. \tag{20}$$

Only the real part, thereof, has the physical meaning (the imaginary part has no physical interpretation for this example). The second equation derived can be rewritten in the following form

$$\lambda_{rr}\frac{1}{r}\frac{\partial}{\partial r}\left(r\frac{\partial\vartheta}{\partial r}\right) + \lambda_{\alpha\alpha}\frac{1}{r^2}\frac{\partial^2\vartheta}{\partial\alpha^2} - c_\mathrm{p}\rho\dot{\vartheta} = -P. \tag{21}$$

Both temperature functions $\vartheta(r)$, $\theta(r)$ must fulfil the relation

$$T(r,\alpha,t) = \mathrm{Re}\{\theta(r)e^{2ix}\} + \vartheta(r). \tag{22}$$

Physical interpretation of both temperature functions is rather evident. The temperature $\vartheta(r)$ represents the average angular-time (x depends on t and α for $p \neq 0$) temperature component. The second component $\theta(r)$ describes the angle-time change of the physical temperature. The modulus and argument of the complex temperature $\theta(r)$ represents the magnitude and the

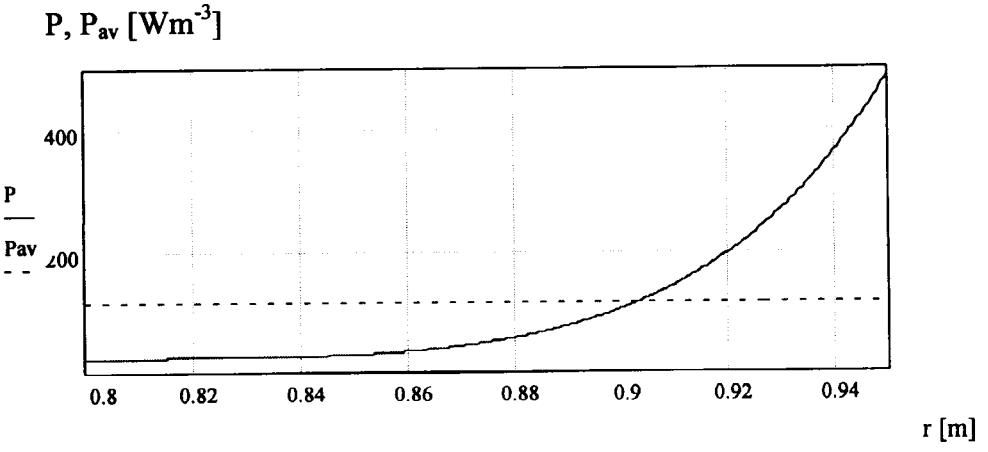

Fig. 2. The power losses density P and its average value P_av [W m^{-3}] vs local radius r [m] for the generator.

phase of temperature oscillations, respectively. The angle-time variation of the temperature for the steady-periodic state of work describes the factor $\exp(2ix)$, which depends on time and angular coordinate. The complex temperature component $\theta(r)$ does not depend on position angle and time for the steady-periodic state of work. The solution (22) is valid for the time points for which all transient terms of the solution had been vanishing. The so-called steady-periodic state solution has been obtained.

The partial time derivative in Eq. (22) for the steady-periodic could be represented as the multiplication of the imaginary operand $2\omega i$ and the complex temperature θ (the real part of it means the physical temperature) as follows:

$$\frac{\partial}{\partial t}\theta \Longrightarrow 2\omega i\theta.$$

Hence, Eq. (20) takes the form of the inhomogeneous Bessel's equation

$$\frac{1}{r}\frac{\partial}{\partial r}\left(r\frac{\partial\theta}{\partial r}\right)-\left(\frac{\lambda_{\alpha\alpha}}{\lambda_{rr}}\frac{p^2}{r^2}+\kappa^2\right)\theta=-\frac{\Delta P(r)}{\lambda_{rr}}. \tag{23}$$

which for $\Delta P(r)\equiv 0$ leads to the homogeneous Bessel's equation of p_Tth order with the following solution [6]:

$$\theta(r)=a_\theta I_{pT}(\kappa r)+b_\theta K_{pT}(\kappa r). \tag{24}$$

For the solid rotor $a=R$, the constant b_θ must vanish due to infinity value of modified Bessel's function $K_{pT}(\kappa r)$ for $r\to 0$, then Eq. (25) yields

$$\theta(r)=a_\theta I_{pT}(\kappa r). \tag{25}$$

The second order Bessel's Eq. (23) can be written in matrix form as follows [6]

$$\mathbf{X}'(r)+\mathbf{A}(r)\mathbf{X}(r)=\mathbf{P}(r). \tag{26}$$

where it was denoted

$$\mathbf{X}(r)=\begin{bmatrix}\theta(r)\\ \theta'(r)\end{bmatrix},\quad \mathbf{A}(r)=\begin{bmatrix}0 & -1\\ -k(r) & r^{-1}\end{bmatrix},\qquad \mathbf{P}(r)=\begin{bmatrix}0\\ -\Delta P(r)\lambda_{rr}^{-1}\end{bmatrix}. \tag{27}$$

The solution of Eq. (26) has the well-known form

$$\mathbf{X}(r)=\mathbf{W}(r)\mathbf{C}, \tag{28}$$

where

$$\mathbf{W}(r)=\begin{bmatrix}I_{pT}(\kappa r) & K_{pT}(\kappa r)\\ I'_{pT}(\kappa r) & K'_{pT}(\kappa r)\end{bmatrix},\quad \mathbf{C}=\begin{bmatrix}a_\theta\\ b_\theta\end{bmatrix}. \tag{29}$$

The solution of Eq. (23) (or of Eq. (26), equivalently) can be received by the method of constant's variation in the way $a_\theta \Rightarrow a_\theta(r)$ and $b_\theta \Rightarrow b_\theta(r)$. Hence, Eq. (28) takes the form

$$\mathbf{X}(r)=\mathbf{W}(r)\mathbf{C}(r). \tag{30}$$

Substituting the solution given above into Eq. (26) one obtains the general solution in the form given below [6]

$$\mathbf{X}(r)=\mathbf{W}(r)\left[\int_{R-a}^{r}\mathbf{W}^{-1}(r)\mathbf{P}(r)\,\mathrm{d}r+\mathbf{C}_o\right], \tag{31}$$

where the inverse of the Wronsky matrix $\mathbf{W}(r)$ [6] in expanded form becomes

$$\mathbf{W}^{-1}(r)=\det{}^{-1}[\mathbf{W}(r)]\begin{bmatrix}K'_{pT}(\kappa r) & -K_{pT}(\kappa r)\\ -I'_{pT}(\kappa r) & I_{pT}(\kappa r)\end{bmatrix},$$

$$\det[\mathbf{W}(r)]=-\frac{1}{r}. \tag{32}$$

The temperature component $\Theta(r)$ and its radial derivative have the following final form

$$\begin{bmatrix}\theta(r)\\ \theta'(r)\end{bmatrix}=\mathbf{W}(r)\left\{\begin{bmatrix}I_1(r)\\ I_2(r)\end{bmatrix}+\mathbf{C}_o\right\}, \tag{33}$$

where two auxiliary integrals have been defined

$$I_1(r)=\lambda_{rr}^{-1}\int_{R-a}^{r}K_{pT}(\kappa r)\Delta P(r)r\,\mathrm{d}r,\qquad I_2(r)=-\lambda_{rr}^{-1}\int_{R-a}^{r}I_{pT}(\kappa r)\Delta P(r)r\,\mathrm{d}r \tag{34}$$

The second temperature component $\vartheta=\vartheta(r)$ results in the steady-periodic state form Eq. (21)

$$\vartheta(r)=-\int_{R-a}^{r}\frac{\int_{R-a}^{r}P(r)r\,\mathrm{d}r}{\lambda_{rr}r}\,\mathrm{d}r+c_1\ln\left(\frac{r}{R-a}\right)+c_2. \tag{35}$$

According to Eq. (33) and (35), the temperature $T(r,\alpha,t)$ for the steady-periodic regime has the form given below

$$T(r,\alpha,t)=\vartheta(r)+\mathrm{Re}\{e^{2xi}[a_\theta I_{pT}(\kappa r)+b_\theta K_{pT}(\kappa r)+I_{pT}(\kappa r)I_1(r)+K_{pT}(\kappa r)I_2(r)]\}. \tag{36}$$

The boundary conditions for the temperature $T(r,\alpha,t)$ take the forms given below [5]:

- the continuity of the flux at the boundary layer—ferromagnetic core ($r=R-a$, $x\in[0,2\pi]$) for the steady-periodic state of work is described by the fol-

lowing relation

$$\frac{\partial T}{\partial r} = 0. \tag{37}$$

It is due to the fact that the heat flux does not flow into the core. Namely, the converters core is insulated from the anisotropic layer for not conducting both electric current and heat flux into core region. The surface $r = R - a$ introduces adiabatic condition for heat transfer and condition of isolation for electric current, respectively.

- the convection phenomenon on the layer—the gap ($r = R, x \in [0, 2\pi]$) boundary leads to

$$-\lambda_{rr}\frac{\partial T}{\partial r} = \alpha_f(T - T_f), \tag{38}$$

where the convection coefficient [8] is assumed to be independent from the temperature.

For $r = R - a$, both auxiliary integrals vanish, hence according to the boundary condition (37) and Eq. (36) two equalities are satisfied

$$c_1 = 0 \quad \text{and} \quad b_\theta = -a_\theta S_T = -a_\theta \frac{I'_{PT}(\kappa r)}{K'_{PT}(\kappa r)}|_{r=R-a}. \tag{39}$$

For $r = R$, according to the boundary condition (38) and Eq. (36) it holds

$$c_2 = T_f + \frac{\int_{R-a}^{R} P(r) r \, dr}{\alpha R} + \int_{R-a}^{R} \frac{\int_{R-a}^{r} P(r) r \, dr}{\lambda_{rr} r} dr, \tag{40}$$

and

$$a_\theta = -\frac{\lambda_{rr}\alpha^{-1}\{I'_{PT}(\kappa R)I_1 + K'_{PT}(\kappa R)I_2\} + I_{PT}(\kappa R)I_1 + K_{PT}(\kappa R)I_2}{\lambda_{rr}\alpha^{-1}\{I'_{PT}(\kappa R) - S_T K'_{PT}(\kappa R)\} + I_{PT}(\kappa R) - S_T K_{PT}(\kappa R)}. \tag{41}$$

where it was denoted

$$I_1 = I_1(R), \quad I_2 = I_2(R). \tag{42}$$

Having determined Bessel's functions they can be used in conjunction with a computer programme for the temperature evaluation. The relations (39), (40) and (41) enable one to calculate all necessary constants which appeared in the solution (36). Both temperature and its radial derivative can be calculated for the steady-periodic regime for every point of the layer of the electromechanical converter considered.

The distribution of temperature and heat flux vs radius and position angle have been shown in Figs. 2–5. The spatial variation of the temperature T (solid line) has been compared with T_{av} temperature distribution (dashed line) calculated as if the power losses density would not depend on both of the coordinates (r, α). The overall values of the power losses are the same for both the temperature distributions (Fig. 2). All values have been denoted for SI units. The calculations with the help of Mathcad software to a tolerance of 10^{-25} have been provided. For controlling the accuracy of solution obtained the boundary conditions Eqs. (37) and (38) have been checked. The boundary condition at $r = R - a$ for zero temperature gradient (37) with the accuracy at leat 10^{-14} K m^{-1}, and the condition (38) with relative accuracy 10^{-8}, respectively (Table 4).

6. Discussion of the results

The calculation has been provided for the material parameters given in Tables 2 and 3. The isotropic case could be obtained as a particular case. Assuming, $p = 0$ the currents and magnetic field do not vary with the position angle, the case of electric current flow is gained analogously and presented in [1] where the electrical field is exerted in a different way than in this paper. For such a case the calculations used for Bessel's function are 0th order for the temperature and first order for the temperature derivative. Since $p > 0$, the Bessel's function order is positive ($p_T > 0$) and is either even for isotropic ($\lambda_{\alpha\alpha} = \lambda_{rr}$) rotor or for anisotropic ($\lambda_{\alpha\alpha} \neq \lambda_{rr}$) rotor uneven.

The fulfilment of boundary conditions (37) and (38) has been checked for all cases (see Table 4). Hence, one can state that the solutions are unique. Moreover, the temperature distribution and its partial radial derivative have been put into Eqs. (19) and (20).

From the results presented, it is apparent that the temperature varies significantly with the radial coordinate. The maximum of the temperature appears near the outer surface of the rotor. It is due to the increase of the losses density vs the radius (see Fig. 2). For accurate calculations the change of the power losses volume density should be taken into account (Figs. 3 and 4). If neglected, the temperature of the rotor is almost invariable. In Fig. 2 the rise of the power losses density is shown. In the cases shown in Figs. 3 and 4

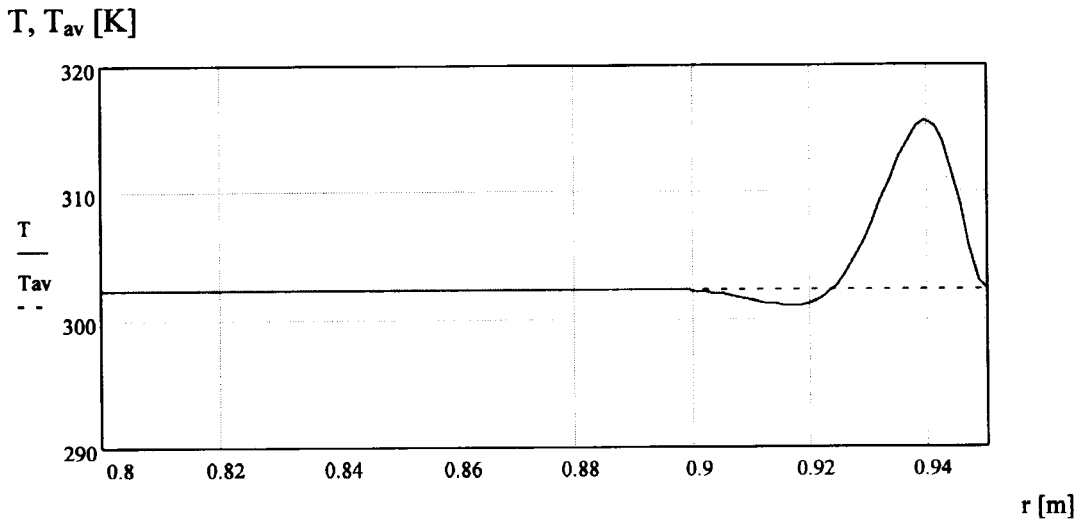

Fig. 3. The layer temperature T [K] distribution (solid line) for real power distribution and T_{av} for average distribution of power (dashed line) vs radius r [m] for the generator.

the maximum temperature appears inside the rotor region. The greater convection coefficient between the rotor surface and air-gap, the smaller the radius is at which the maximum temperature appears in layer. The appropriate to the Fig. 3 temperature distribution in Fig. 5 heat flux vs radius has been shown. In Fig. 6 the maximal layer temperature vs anisotropy coefficient $k=\lambda_{rr}/\lambda_{\alpha\alpha}\in(0.75,\ 1.25)$ has been presented. The maximum maximorum thereof appears for $\lambda_{rr}<\lambda_{\alpha\alpha}$. In conjunction with the rise of radial thermal conductivity increases the heat flux in radial direction. This leads to the most intensive heat transfer and decreasing of the maximal temperature in rotor.

7. Conclusion

For the electromechanical converters considered, the distribution of the magnetic vector potential, electric field strength and temperature inside the solid and anisotropic rotor have been evaluated. Both the stator and rotor currents as the sources of the losses have

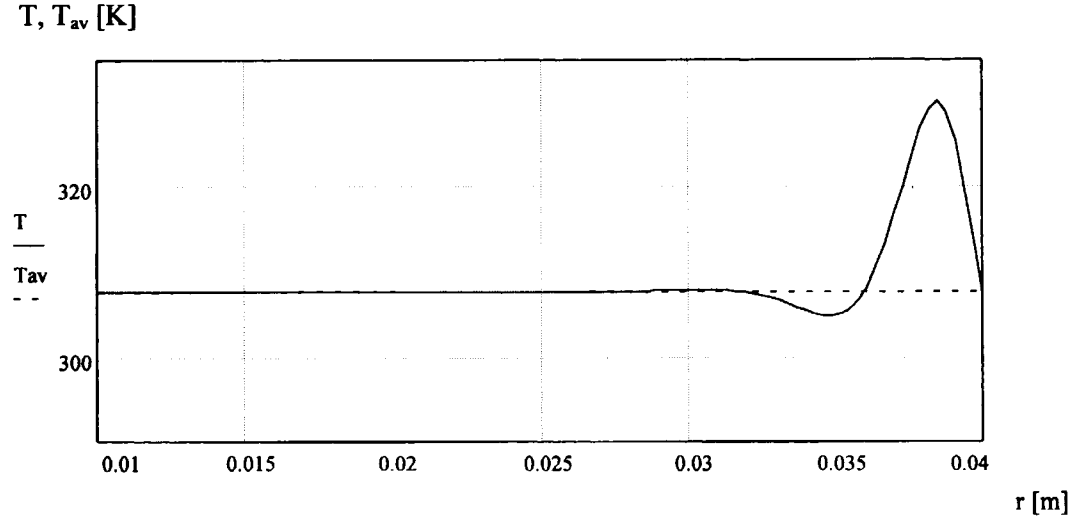

Fig. 4. The layer temperature T [K] distribution (solid line) for real power distribution and T_{av} for average distribution of power (dashed line) vs radius r [m] for two-phase machine.

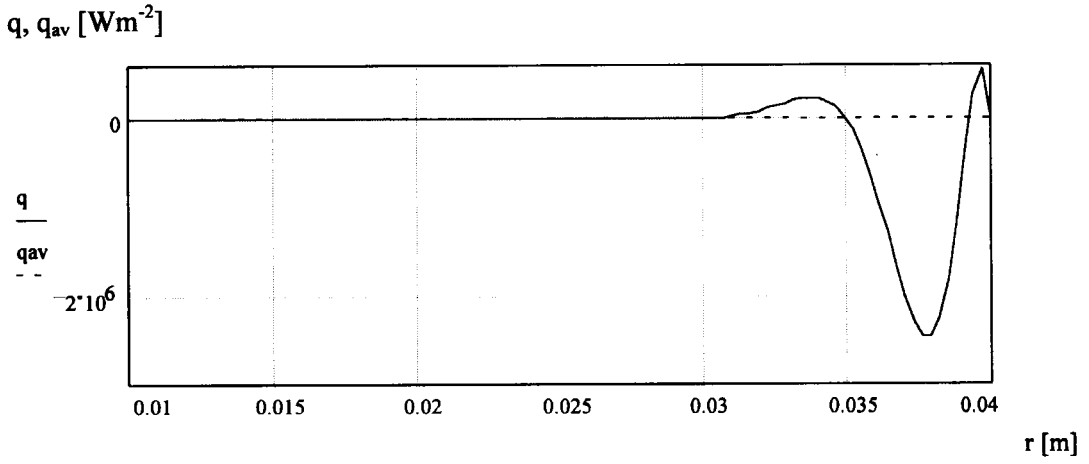

Fig. 5. The heat flux density radial component q [W m^{-2}] and heat q_{av} calculated for average distribution of power (dashed line) vs radius r [m] for two-phase machine.

Table 2
Electromagnetic and thermal parameters for the power-station generator

Parameters	Electromagnetic	Thermal	The forced
The gap $R=0.95$ m $g=0.012$ m	$\nu_o=(1/4\pi)\cdot 10^7$ H m^{-1}	–	$\alpha_f=1.3$ W m^{-2} K^{-1}, $T_f=290$ K, $\theta_s=1000$ A, $p=2$
The layer $a=0.15$ m	$\nu_{rr}=0.05\nu_o$, $\nu_{\alpha\alpha}=0.07\nu_o$, $\gamma=2\cdot 10^6$ S m^{-1}	$\lambda_{rr}=90$ W (m K)$^{-1}$, $\lambda_{\alpha\alpha}=120$ W (m K)$^{-1}$, $c_p=50$ J (kg K)$^{-1}$, $\rho=2.4\cdot 10^{-3}$ kg (m)$^{-3}$	$s=2\pi\cdot 2i$ rad s^{-1}
The core	$\nu_{Fe}=0$	$\lambda_{Insulation}\rightarrow 0$	–

Table 3
Electromagnetic and thermal parameters for the 2-phase machine

Parameters	Electromagnetic	Thermal	The forced	
The gap $g=0.0007$ m $R=0.04$ m	$\nu_o=(1/4\pi)\cdot 10^7$ H m^{-1}	–		$\alpha_f=0.3$ W m^{-2} K^{-1}, $T_f=290$ K, $\theta_s=50$ A, $p=1$
The layer $a=0.03$ m	$\nu_{\alpha\alpha}=0.03\nu_o$, $\nu_{rr}=0.05\nu_o$, $\gamma=1.3\cdot 10^7$ S m^{-1}		$\lambda_{rr}=143$ W (m K)$^{-1}$, $\lambda_{\alpha\alpha}=163$ W (m K)$^{-1}$, $c_p=135$ J (kg K)$^{-1}$, $\rho=1.9\cdot 10^4$ kg (m)$^{-3}$	$s=2\pi\cdot 5i$ rad s^{-1}
The core	$\nu_{Fe}=0$	$\lambda_{Insulation}\rightarrow 0$		–

Table 4
Boundary conditions (37) and (38) fulfilment

Parameters	Electromagnetic	Thermal	Boundary condition
The gap $R=0.95$ m $g=0.012$ m	$\nu_o=(1/4\pi)\cdot 10^7$ H m^{-1} $\omega\epsilon_o\gamma^{-1}=5.6\cdot 10^{-17}$	$Bi=0.01$	for $r=R-a$ $\lvert\frac{\partial T}{\partial r}\rvert<10^{-14}\frac{K}{m}$
The layer $a=0.15$ m	$\nu_{rr}=0.05\nu_o$, $\nu_{\alpha\alpha}=0.07\nu_o$, $\gamma=2\cdot 10^6$ S m^{-1} $\beta R=20.18$ $p_B=1.69$	$\lambda_{rr}=90$ W (m K)$^{-1}$, $\lambda_{\alpha\alpha}=120$ W (m K)$^{-1}$, $c_p=50$ J (kg K)$^{-1}$, $\rho=2.4\cdot 10^3$ kg (m)$^{-3}$ $\kappa R=173.9$ $p_T=2.31$	for $r=R$ $\frac{\lambda_{rr}}{\alpha_f(T-T_f)}\frac{\partial T}{\partial r}=0.999999995$
The core	$\nu_{Fe}=0$	$\lambda_{Insulation}\to 0$	

been taken into account. The paper extends the work [1] wherein Barletta and Zanchini have determined analytically the steady-periodic temperature for two-layered solid isotropic annular conductor $\lambda_{\alpha\alpha}=\lambda_{rr}$, $\nu_{\alpha\alpha}=\nu_{rr}=\nu_o=(\mu_o)^{-1}$ resistor, crossed by the alternating current with zero-pair pole $p=0$ (skin effect). In this paper the anisotropy and rotation of the rotor have been taken into account. The temperature and heat flux have been determined for the region of anisotropic machine rotor, where the measurements cannot be easily provided. The transient and nonlinearity have been neglected.

The solution in a relatively simple way has been obtained for the set of known material and geometrical parameters for particular electromechanical converter.

The analytical solution has been determined while considering the following phenomena:

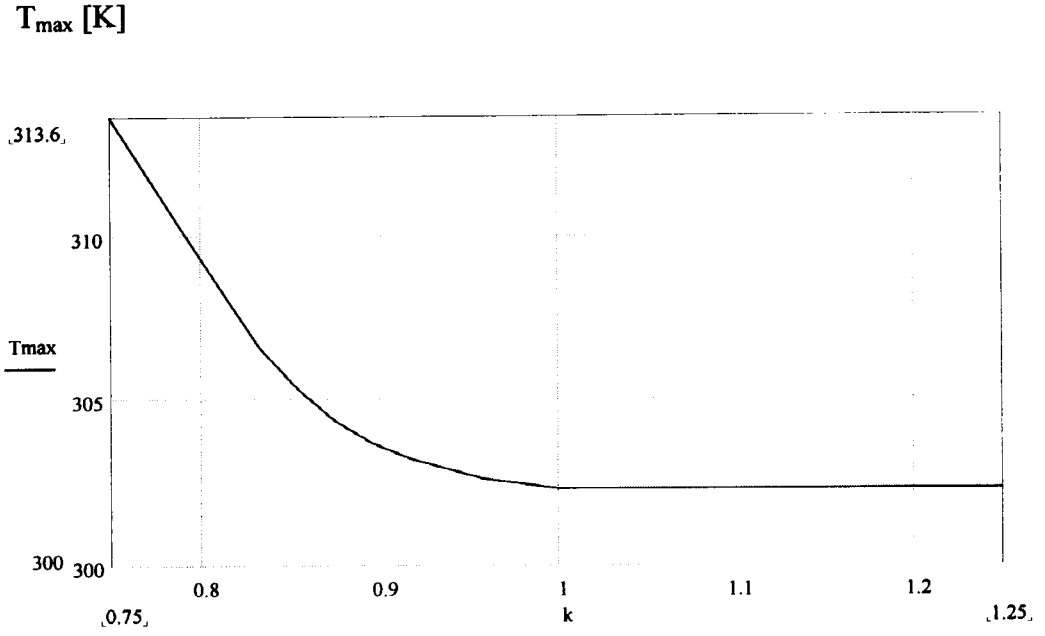

Fig. 6. The maximal temperature T_{max} [K] of anisotropic rotor for generator vs thermal conductivity ratio $k=\lambda_{rr}/\lambda_{\alpha\alpha}\in(0.75, 1.25)$ for $\lambda_{\alpha\alpha}=120$ [W m^{-1} K^{-1}].

1. the rotation of electromechanical converter rotor;
2. two-dimensional temperature distribution;
3. the rotor temperature dependence on time for steady-periodic state of work;
4. the flow of the currents forced by both the stator and rotor current;
5. the diagonal anisotropy of material parameters.

The obtained results can easily be used for temperature and heat flux determination at design process for both the power-station generators and small induction machines with anisotropic, conducting rotor. The way of analysis derived could be incorporated into the list of the methods useful for evaluation of temperature rise in electromechanical coverters.

Appendix

There are defined boundary conditions of continuity for:

• the tangential (angular) components at the boundary of the stator—the stator windings—the air-gap ($r = R + g = R_g$):

$$\nu_o B_{\delta\alpha} = -\frac{1}{R_g}\frac{\partial \Theta_s}{\partial \alpha} \Longrightarrow a_\delta (R_g)^{p-1} - b_\delta (R_g)^{-p-1} = \Theta_s/(R_g \nu_o),$$

• the normal (radial) components at the boundary of the air-gap—the layer ($r = R$);

$$B_{\delta r} = B_{ar} \Longrightarrow a_\delta R^p + b_\delta R^{-p} = a_a I_{pB}(\beta R) + b_a K_{pB}(\beta R),$$

• the tangential (angular) components at the boundary of the air-gap—the layer ($r = R$):

$$\nu_o B_{\delta\alpha} = \nu_{\alpha\alpha a} B_{a\alpha} \Longrightarrow \nu_o p\{a_\delta R^{p-1} - b_\delta R^{-p-1}\} = \nu_{\alpha\alpha}\beta\{a_a I'_{pB}(\beta R) + b_a K'_{pB}(\beta R)\},$$

• the tangential (angular) components at the boundary of the layer—the core $r = R - a = R_a$:

$$\nu_{\alpha\alpha} B_{a\alpha} = 0 \Longrightarrow a_a I'_{pB}(\beta R_a) + b_a K'_{pB}(\beta R_a) = 0.$$

The four conditions derived above enable one to determine the four constants

$$a_a = \Theta_s \nu_o^{-1}\{U(R_g)^p - W(R_g)^{-p}\}^{-1},$$

$$b_a = -a_a \frac{I'_{pB}(\beta R_a)}{K'_{pB}(\beta R_a)} = -a_a S,$$

$$a_\delta = a_a U, \quad b_\delta = a_a W,$$

where it was denoted for simplification

$$U = 0.5(R^{-p+1}P + R^{-p}Q), \quad W = 0.5(-R^{p+1}P + R^p Q),$$

$$P = \frac{\beta \nu_{\alpha\alpha}}{p\nu_o}\{I'_{pB}(\beta R) - SK'_{pB}(\beta R)\},$$

$$Q = I_{pB}(\beta R) - SK_{pB}(\beta R).$$

References

[1] A. Barletta, E. Zanchini, The temperature field in cylindrical electric conductor with annular section, Int. J. Heat Mass Transfer 38 (1995) 2821–2832.

[2] J. Golębiowski, S. Kwiećkowski, Analytical and numerical modelling of a stationary temperature field in a three-dimensional electric heating system, Electrical Engineering 81 (1998) 69–76.

[3] P.C. Krause, Analysis of Electric Machinery, McGraw-Hill Book Company, USA, 1986.

[4] L.D. Landau, E.M. Lifszyc, The Classical Theory of Fields, Pergamon, New York, 1961.

[5] J. Sucec, Heat Transfer, Wm C Brown, 1995.

[6] R. Rothe, I. Szabo, Higher Mathematics, BG Teubner Verlagsgesellschaft, Stuttgart, 1965.

[7] Da Yu Tzou, The anisotropic overall thermal conductivity induced by preferentially oriented pores, Int. J. Heat Mass Transfer 38 (1995) 23–30.

[8] L.C. Woods, The Thermodynamics of Fluid Systems, Clarendon Press, Oxford, 1975.

[9] L.C. Wróbel, C.A. Brebia, A formulation of the boundary element method for axisymmetric transient heat conduction, Int. J. Heat Mass Transfer 24 (1981) 843–850.